Report on practical use of the asymptotic formulas

S. Chevillard

May 24, 2017

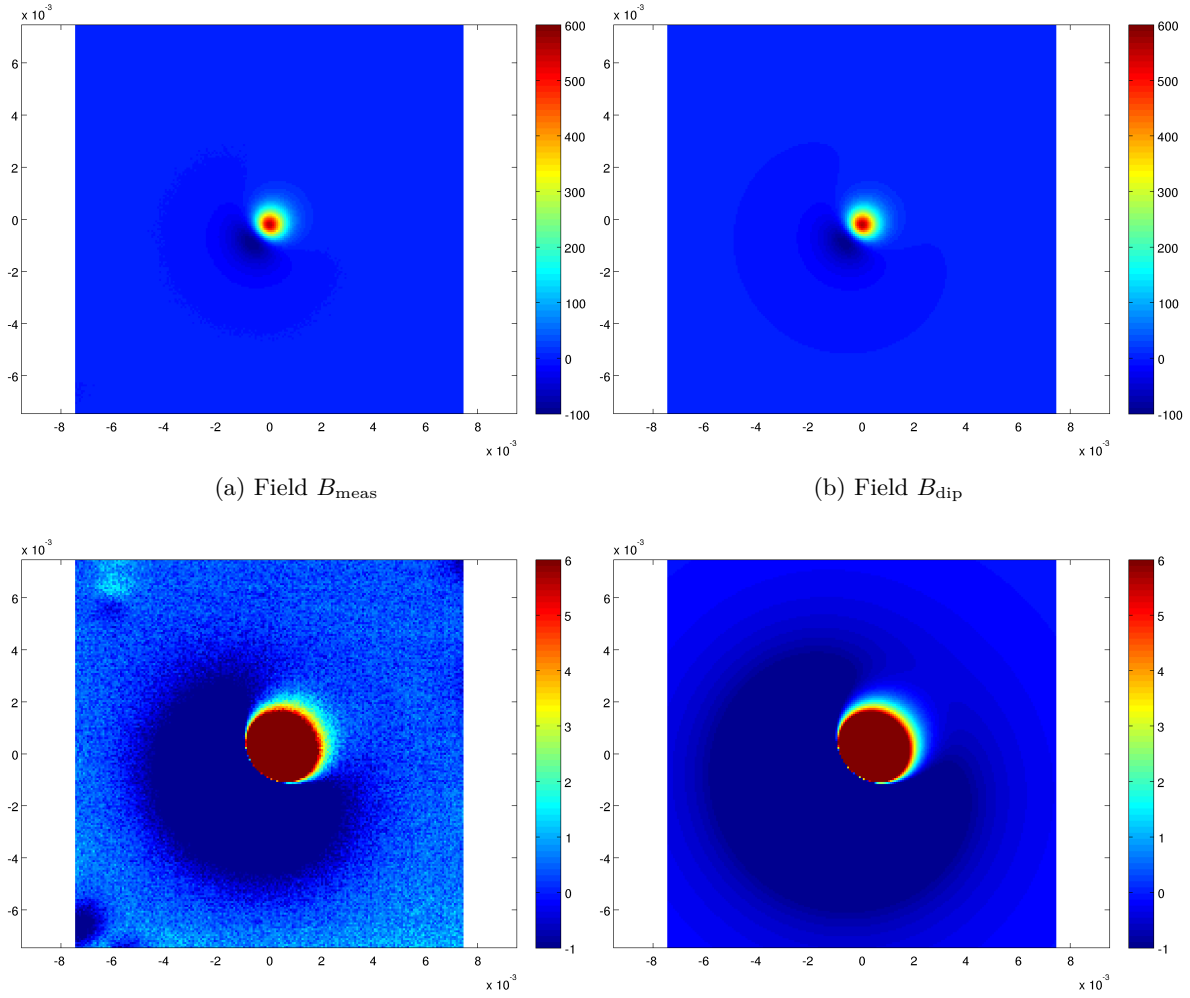

(a) Field B_{meas}

(b) Field B_{dip}

(c) Field B_{meas}, saturated color scale

(d) Field B_{dip}, saturated color scale

Figure 1: Measured and synthetic field maps.

We consider here the field B_{meas} from `LONJ_NRM_10k_liftoff_675um.mat`. It corresponds to the lonar spherule, measured at a higher height than usual. It contains 200×200 points with a step δ of 75 microns. By convention, we fix the origin of the horizontal plane at the center of the map, *i.e.*, the map corresponds to the square $[-0.0075, 0.0075] \times [-0.0075, 0.0075]$.

Based on a dipole fitting made by Eduardo, we also consider the field B_{dip} generated by a dipole at height $h = 835.38$ microns under the measurement plane and located at

$(-1.5020\,\mathrm{e}{-4}, -3.7910\,\mathrm{e}{-4})$ on the horizontal plane. The moment of the dipole has inclination 41.7362 degrees, declination 316.3451 degrees and magnitude 2.056. In cartesian coordinates, the moment is hence $(1.0591, 1.1100, 1.3687)$. Both fields are fairly similar as can be seen on Figure 1.

1 The asymptotic formulas in a nutshell

Let us denote with Q_R the square $[-R, R] \times [-R, R]$ and with D_R the diamond inscribed in Q_R (*i.e.*, the square whose vertices are the middle of the edges of Q_R). The SQUID microscope does not truly measure the field, but actually the field plus some unknown constant β. The asymptotic formulas that we have been using so far give (with i being 1 or 2):

$$\iint_{\mathbb{R}^2} \frac{2(\sqrt{2}\chi_{Q_R}(x_1,x_2) - \chi_{D_R}(x_1,x_2))}{\mu_0(\sqrt{2}-1)}\, x_i\, (B_3(x_1,x_2)+\beta)\,\mathrm{d}x_1\,\mathrm{d}x_2 = \langle m_i\rangle + \mathcal{O}(1/R^3), \quad (1)$$

$$\iint_{\mathbb{R}^2} \frac{\pi\, R(\chi_{Q_R}(x_1,x_2) - 2\chi_{D_R}(x_1,x_2))}{\mu_0(\sqrt{2}-4)}\, (B_3(x_1,x_2)+\beta)\,\mathrm{d}x_1\,\mathrm{d}x_2 = \langle m_3\rangle + \mathcal{O}(1/R^2). \quad (2)$$

The term β is not a problem for recovering $\langle m_1\rangle$ and $\langle m_2\rangle$ because it is killed by integration against x_i. The linear combination of χ_{Q_R} and χ_{D_R} allows us here to kill the $\mathcal{O}(1/R)$ that would normally come after the constant term, and hence increase the speed of convergence to $1/R^3$ (because the $1/R^2$ term turns out to be 0 in the asymptotic expansion anyway). However, the term β is a problem for recovering $\langle m_3\rangle$ as it introduces a term of order R^3 before the constant term in the expansion. The linear combination of χ_{Q_R} and χ_{D_R} is here designed to kill that term.

2 Synthetic vs measured example

The result of applying these formulas on B_{meas} and B_{dip}, as a function of R is shown on Figure 2.

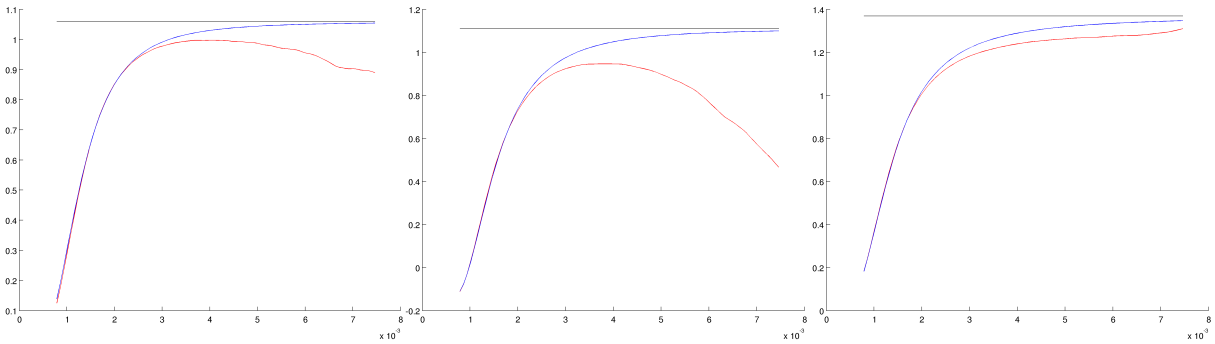

(a) Estimate of $\langle m_1\rangle$ (b) Estimate of $\langle m_2\rangle$ (c) Estimate of $\langle m_3\rangle$

Figure 2: Estimates provided by Equations (1) and (2), as a function of R. The red curve corresponds to the field B_{meas}, the blue curve corresponds to the field B_{dip} and the black line corresponds to the true value $\langle m_i\rangle$.

For each of the three components, one can distinguish three regions:

- At start, both fields lead to pretty much the same estimate. However, this estimate is a bad approximation of the corresponding $\langle m_i\rangle$, because we are still far from the asymptotic regime.

- Then, the estimates of both fields start diverging one from another. Namely, the estimate based on the synthetic dipolar field seems to converge to the true value, while the estimate based on the measured field diverges, but somehow smoothely. This only affects $\langle m_1 \rangle$ and $\langle m_2 \rangle$.
- Finally, the estimate based on the measured field ends up having a not so smooth behavior, due to the noisy features near the edges of the measurement area.

The first question we addressed was: why is the estimate based on the true measurements diverging from the synthetic one, even though both fields look the same? Eduardo came up with a suggestion: the SQUID has a natural drift with time, and since it scans a row after another this introduces a noise which is small but with a mean value which is not zero. Even if the effect on the field is small, this might affect the behavior of the formulas, since they are integrating it, exactly as with the constant β.

Let us assume that the SQUID is measuring one point after another at constant speed, with some fixed time τ to come back from the end of a row to the start of the following row. Also, let us assume that its drift is roughly a linear function of the time during the experiment. Then, assuming for instance that the SQUID measures the field succesively at points $(x[1], y[1])$, $(x[2], y[1])$, $\ldots$, $(x[200], y[1])$, $(x[1], y[2])$, $(x[2], y[2])$, $\ldots$, $(x[200], y[200])$, we see that the drift at point $(x[k], y[j])$ is $((200 + \tau)(j-1) + (k-1))\alpha$, where α is the drift during one unit of time. Now, since $y[j] = y[1] + (j-1)\delta$ and $x[k] = x[1] + (k-1)\delta$, we see that the measured field at point (x, y) is indeed of the form $B_3(x, y) + \gamma x + \gamma' y + \beta'$. The term β' is already handled by the formulas as explained above. The terms γx and $\gamma' y$ do not affect the estimate of m_3 because they are killed by integration. However, they affect the estimate of $\langle m_1 \rangle$ and $\langle m_2 \rangle$ by introducing a R^4 term before the constant term in the asymptotic expansion. Hence, even if the constants are small, their effect when R grows becomes quickly dominant.

3 Experimenting on the synthetic example

To validate this hypothesis, we form the synthetic field $B_{\text{shift}}(x, y) = B_{\text{dip}}(x, y) - 10x - 35y$.

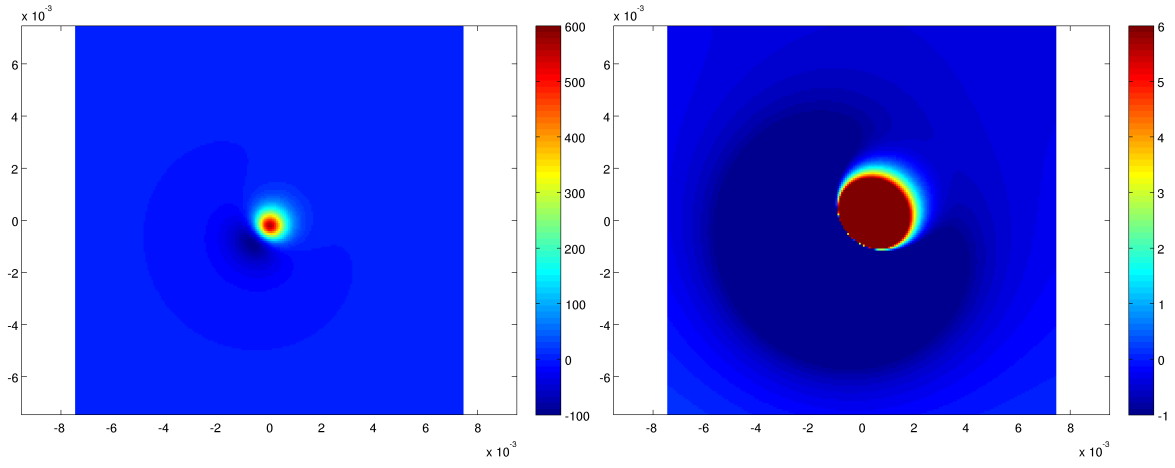

(a) Field B_{shift} (b) Field B_{shift}, saturated color scale

Figure 3: Synthetic field with the modelled drift $-10x - 35y$.

The estimates provided by Equations (1) and (2) on this field are shown on Figure 4. As expected, the estimate for $\langle m_3 \rangle$ has not been affected, whereas the other estimates now also

exhibit a converge-then-diverge pattern. The constants 10 and 35 have been manually chosen so as to obtain the same kind of behavior as with B_{meas}. Yet, **it is an open question for me why we only have a 3.5 ratio between them, when I would expect something of the order 200**.

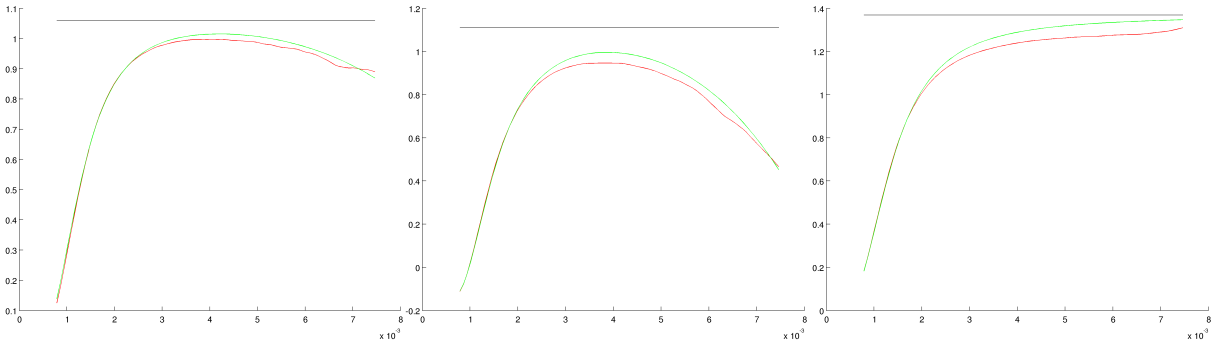

(a) Estimate of $\langle m_1 \rangle$ (b) Estimate of $\langle m_2 \rangle$ (c) Estimate of $\langle m_3 \rangle$

Figure 4: Estimates provided by Equations (1) and (2), as a function of R. The red curve corresponds to the field B_{meas}, the green curve corresponds to the field B_{shift} and the black line corresponds to the true value $\langle m_i \rangle$.

In order to overcome this issue, we can apply the same strategy as what we did for β: instead of using a linear combination of χ_{Q_R} and χ_{D_R} to increase the convergence speed, we can use an appropriate combination to kill the contribution of γ and γ'. Of course, this comes to the price of a convergence back in $1/R$. Namely, we have

$$\iint_{\mathbb{R}^2} \frac{2(-\chi_{Q_R} + 4\chi_{D_R})(x_1, x_2)}{3\mu_0} x_i \left(B_3(x_1, x_2) + \beta + \gamma_1 x_1 + \gamma_2 x_2\right) \mathrm{d}x_1 \, \mathrm{d}x_2 = \langle m_i \rangle + \mathcal{O}\Big(\frac{1}{R}\Big) \quad (3)$$

This is illustrated on Figure 5 where we see on the same graph the estimates obtained on B_{dip} with the original asymptotic formula (1), and on B_{shift} both with Equation (1) and with the new formula (3). We clearly see that the converge-then-diverge pattern disappears. However, the estimate that we get is fairly bad because the convergence is slow.

We can come back to a convergence in $1/R^3$ by using yet another combination of shapes. For instance, a linear combination of χ_{Q_R}, $\chi_{Q_{\lambda R}}$ and Q_{D_R} (for some chosen parameter λ) does the trick. Namely:

$$\iint_{\mathbb{R}^2} \psi(x_1, x_2) \, x_i \left(B_3(x_1, x_2) + \beta + \gamma_1 x_1 + \gamma_2 x_2\right) \mathrm{d}x_1 \, \mathrm{d}x_2 = \langle m_i \rangle + \mathcal{O}(1/R^3), \quad (4)$$

where

$$\psi(x_1, x_2) = 2 \, \frac{(-1 + 4\sqrt{2}\lambda^5)\chi_{Q_R}(x_1, x_2) - 4(\lambda^5 - 1)\chi_{D_R}(x_1, x_2) - ((4\sqrt{2} - 1)\lambda)\chi_{Q_{\lambda R}}(x_1, x_2)}{\mu_0(4(\sqrt{2} - 1)\lambda^5 + (1 - 4\sqrt{2})\lambda + 3)}.$$

Notice that, if λ is too close to 1, this gives a considerable importance to the edges where the ratio signal/noise is usually lowest, while if λ is too close to 0, this assumes that the asymptotic regime has already been reached at λR, which requires R to be fairly large. Figure 6 shows the estimates obtained with Equation (4) when $\lambda = 2/3$.

The convergence seems to be slower with this new formula than with the original formula when it was applied to B_{dip}. Actually, the convergence rate is surprisingly well respected when using Equation (1) on B_{dip} and Equation (3) on B_{shift}. This is indeed less true when using

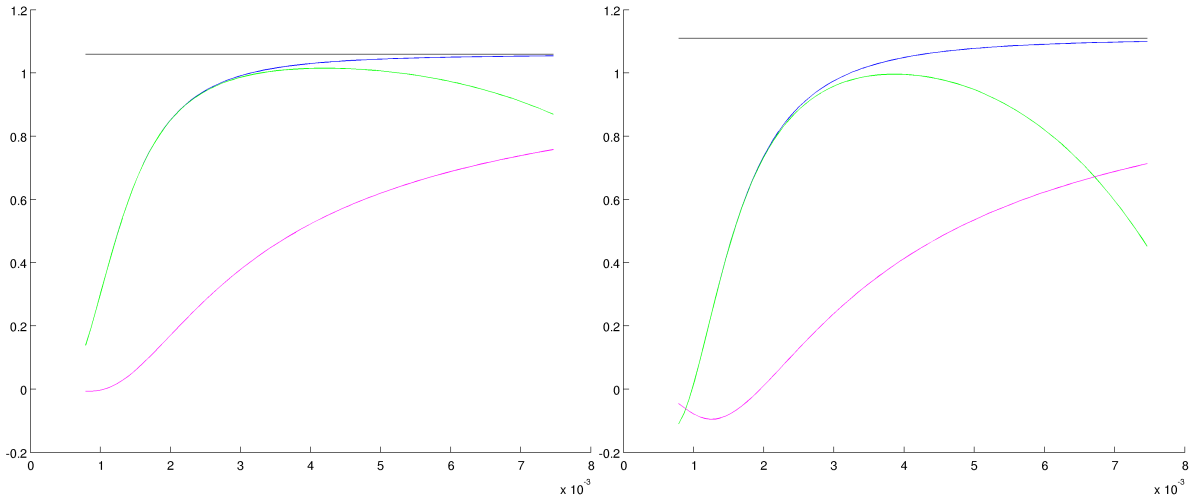

(a) Estimate of $\langle m_1 \rangle$ (b) Estimate of $\langle m_2 \rangle$

Figure 5: Estimates provided by Equation (1) on B_{dip} (blue curve) and on B_{shift} (green curve), and estimate provided by Equation (3) on B_{shift} (purple curve), as functions of R.

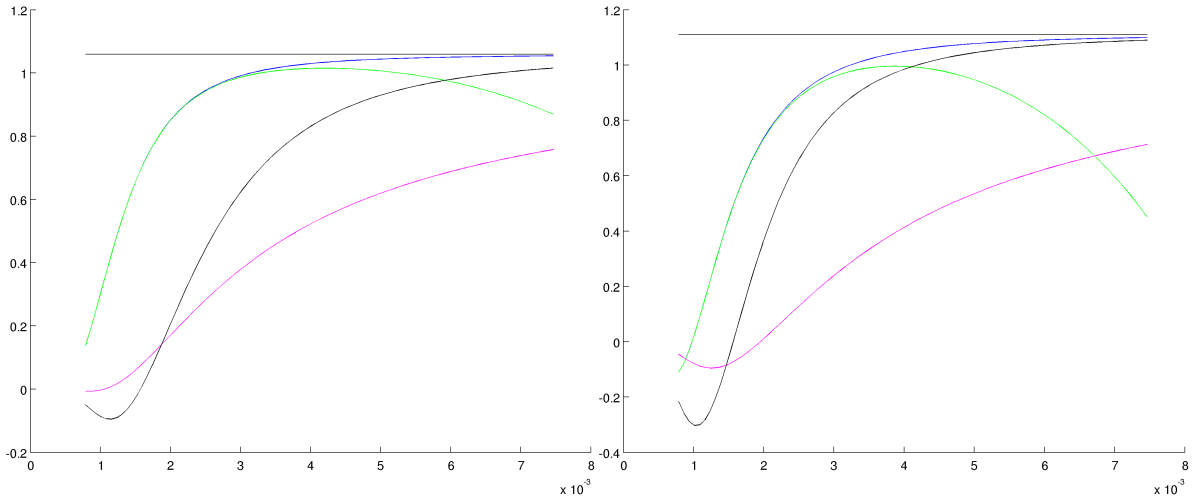

(a) Estimate of $\langle m_1 \rangle$ (b) Estimate of $\langle m_2 \rangle$

Figure 6: Estimates provided by Equation (1) on B_{dip} (blue curve) and on B_{shift} (green curve), provided by Equation (3) on B_{shift} (purple curve), and by Equation (4) on B_{shift} (black curve), as functions of R.

Equation (4) on B_{shift}. On Figure 7, we show in red the result of a least square fitting of the portion of the curve between the two circled points by a function of the form $a + b/R^3 + c/R^4$ in the case of formulas (1) and (4) and by a function of the form $a + b/R + c/R^3$ in the case of formula (3). In any case, the fit is quite good in the region where it is applied and it is indeed very predictive of the subsequent behavior of the curve.

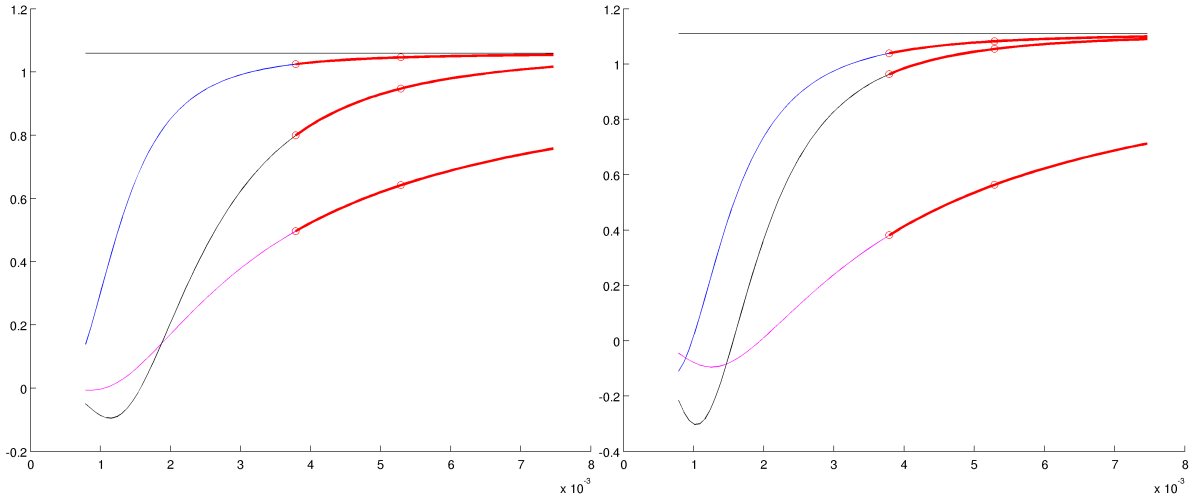

(a) Estimate of $\langle m_1 \rangle$ (b) Estimate of $\langle m_2 \rangle$

Figure 7: Estimates of Figure 6, together with their fitting (in red). The fit is performed only between the circled points. One sees that the fits keep being good further away.

Actually, the fitting turns out to be so good that it is a very efficient way of estimating the limit. The following tables sums up the estimate obtained for $\langle m_1 \rangle$ and $\langle m_2 \rangle$ with each method, either by simply considering the estimate obtained for $R = 0.0075$ (the highest available value for R) or by extrapolating the curve up to its limit at infinity. For $\langle m_3 \rangle$, the estimate at $R = 0.0075$ is 1.3475 and the extrapolated limit (when fitting with a function of the form $a + b/R^2 + c/R^4$, which is the expected form of the asymptotic expansion) gives 1.3696, the true value being 1.3687.

	at $R = 0.0075$	extrapolated
B_{dip} with Equation (1)	1.0547	1.0593
B_{shift} with Equation (3)	0.7583	1.0578
B_{shift} with Equation (4)	1.0162	1.062

Figure 8: Several estimates of $\langle m_1 \rangle$ (true value is 1.0591)

	at $R = 0.0075$	extrapolated
B_{dip} with Equation (1)	1.1102	1.1105
B_{shift} with Equation (3)	0.7136	1.1048
B_{shift} with Equation (4)	1.0905	1.1119

Figure 9: Several estimates of $\langle m_2 \rangle$ (true value is 1.1100)

The conclusion that we can draw from this synthetic example is that we manage to remove a

drift of the form $\gamma x + \gamma' y$ by combining the asymptotic expansion on two shapes. The obtained estimate converges much slower and is fairly bad for the largest value of R that we have. However, the estimate converges precisely as predicted, which allows us to recover a fairly good estimate of the true value, by fitting the curve and looking at the value of the fit at infinity. We can also combine three shapes to recover a better converging rate for the estimate. This is indeed giving a much better estimate at $R = 0.0075$ and a comparable estimate as with the other formulas, when fitting the curve.

4 Applying the method on experimental data

Let us now apply this strategy on the true experimental data B_{meas}. Using the same convention as before, this leads to Figure 10.

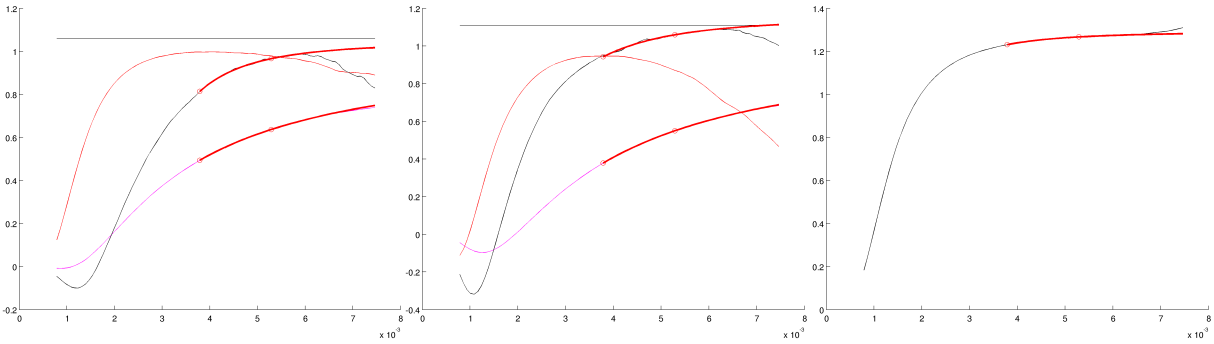

(a) Estimate of $\langle m_1 \rangle$ (b) Estimate of $\langle m_2 \rangle$ (c) Estimate of $\langle m_3 \rangle$

Figure 10: Estimates provided by Equation (1) (red curve), by Equation (3) (purple curve) and Equation (4) (black curve), together with their fits, on the field B_{meas}. The estimate of $\langle m_3 \rangle$ on the last figure, given by Equation (2) is in black.

Formula (4) is still diverging a little bit at the end, but this might be due to the noisy features on the edges of the measured map, more than to a bad modelling or bad correction of the drift of the SQUID.

The estimates for $\langle m_1 \rangle$ and $\langle m_2 \rangle$ obtained by extrapolating the fits are reported in the following tables. As for $\langle m_3 \rangle$, the extrapolation gives 1.2953 (while the estimate at $R = 0.0075$ is 1.3105) to be compared to the value estimated by Eduardo which is 1.3687.

	extrapolated
B_{meas} with Equation (3)	1.0333
B_{meas} with Equation (4)	1.0425

Figure 11: Several estimates of $\langle m_1 \rangle$ (value estimated by Eduardo is 1.0591)

	extrapolated
B_{meas} with Equation (3)	1.0489
B_{meas} with Equation (4)	1.1489

Figure 12: Several estimates of $\langle m_2 \rangle$ (value estimated by Eduardo is 1.1100)

Notice that the values estimated by Eduardo are those obtained with a dipole fitting. We have seen with the synthetic dipolar field that these values are plausible, but it might be that the estimates obtained above with the asymptotic formulas be indeed closer to the true moment than what these values suggest.